Fiber microaxicons fabricated by a polishing technique for the generation of Bessel-like beams

T. Grosjean, S. Sadat Saleh, M.A. Suarez, I. Abdoulkader Ibrahim, V. Piquerey, D. Charraut, P. Sandoz

Fiber microaxicons fabricated by a polishing technique for the generation of Bessel-like beams

Thierry Grosjean,* Said Sadat Saleh, Miguel Angel Suarez, Idriss Abdoulkader Ibrahim, Vincent Piquerey, Daniel Charraut, and Patrick Sandoz

Institut FEMTO-ST, UMR CNRS 6174, Université de Franche-Comté, 16 Route de Gray, 25030 Besançon Cedex, France

*Corresponding author: thierry.grosjean@univ-fcomte.fr

We report a simple method for generating microaxicons at the extremity of commercial optical fibers. The proposed solution, based on a polishing technique, can readily produce any desired microaxicon cone angle and is independent of the nature of the fiber. An optical study of microaxicon performance, in terms of confinement ability and length of the generated Bessel-like beams, is presented as a function of the microaxicon angle. This study, made possible by the experimental acquisition of the 3D light distribution of the Bessel-like beams, reveals the relationship between the Bessel-like beam confinement zone and the beam length. Finally, the effect of diffraction of the Bessel-like beams, induced by the limited lateral extent of the incident fiber mode, is studied and discussed.

1. Introduction

For 20 years, Bessel beams [1,2] have drawn increasing interest in various domains such as optical acceleration [3,4], particle guiding [5] and manipulation [6,7], nonlinear optics [8–14], optical interconnection and alignment [15,16], imaging [17], microfabrication [18], and lithography [19]. Given their high efficiency and the versatility with which they can be used, axicons [20–22] are a valuable tool for generating Bessel beams. The engineering of microaxicons is highly desirable in the context of system miniaturization. The integration of microaxicons at the extremity of optical fibers offers the possibility of producing Bessel-like beams with a compact system that is easy to manipulate. Since such a fiber microaxicon (FIMAX) is centered with respect to the core axis, the use of this component is straightforward: No adjustments of the system are required before use. Such a styluslike device could extend the field of applications of Bessel beams to endoscopy, surgery, the biomedical domain, optical tweezers in turbid media, data storage, and beyond.

So far, two fabrication techniques of FIMAXs have been reported. The first one consists of chemically etching a cleaved optical fiber [23,24]. Although such a method provides axially symmetric conical lenses aligned to the fiber core, the required chemical processes are difficult to master and can suffer from problems of reproducibility. The second one uses focused ion beam (FIB) technology for machining the output facet of the core into a conical shape [25]. Although the resulting FIMAXs do produce well-defined Bessel-like beams, this technique requires the use of an expensive FIB system that can be difficult to use.

In this article, we propose the fabrication of FIMAXs by a mechanical polishing procedure. This technique is simple, low cost, independent of the kind of fiber used, and reproducible. First, the fabrication procedure is described and discussed. Then, Bessel-like beams produced by various polished FIMAXs integrated on a step-index monomode fiber are experimentally characterized by means of a scanning imaging system. The aim here is to accurately measure the 3D light distribution, in terms of confinement ability and propagation length, as a function of the FIMAX cone angle. Such measurements of the real spatial characteristics defining the generated Bessel-

like beams are of considerable practical interest for future applications. The Bessel beam optical study is carried out for four polished FIMAX cone angles. Finally, the effect of diffraction on the spatial behavior of the Bessel-like beams, due to the micrometer-size incident fiber mode, is studied and discussed.

2. Fiber Microaxicon Fabrication

The polishing procedure used for the generation of the FIMAX is depicted in Fig. 1. The optical fiber is set in rotation around its axis of revolution by means of a chuck connected to an electric motor with a belt. The overall system is mounted onto a rotation–translation stage that allows the fiber to be tilted with respect to the abrasive disk. This way, the cone angle (θ) of the FIMAX is simply defined by the tilt angle ($\theta/2$) of the fiber. The fiber is set smoothly in contact with the spinning disk by means of a high-precision translation stage (with a micrometer screw) in order to generate the conical microlens without damaging the fiber. For this task, the micropositioning of the fiber is controlled with a binocular system to accurately detect the point where the fiber end is just at the level of the abrasive surface. The proposed fabrication technique is derived from the one used in [26] for fabricating near-field fiber probes. It is more versatile than the methods based on chemical etching [24] since it does not depend on the nature of the fiber core and it allows direct definition of the cone angle at will by tilting the fiber.

The fabrication of the FIMAX imposes three conditions on the polishing device. First, the FIMAX centering with respect to the core axis requires fine correction of both the imbalance of the chuck and the wobble of the abrasive disk. Second, the roughness level of the polished conical surface has to be sufficiently low and the cone summit sufficiently sharp to accurately generate Bessel beams. These conditions are satisfied by using an abrasive disk with a diamond grain size of $\sim 1\ \mu$m. Finally, for minimizing the risks of loss of cone-to-fiber centering and for optimizing the production of FIMAXs, the time duration of the polishing procedure should be as short as possible. Considering the smoothness of the abrasive surface required for the polishing process, a short duration implies that only a minimum of material is actually removed. Unfortunately, the direct machining of a FIMAX with a standard 125 μm wide fiber can take more than a couple of hours before ending. To reduce the polishing time, the fiber output end has been preshaped in a spherical form before the polishing process. The hemisphere is easily and rapidly fabricated by a controlled heating–pulling technique of the optical fiber. With such a technique, the microlensing can be combined with the tapering of the fiber to obtain microball lenses whose radii of curvature are only a few micrometers. In this case, the size of the lens is of the same order of magnitude as the diameter of the fiber core of standard monomode fibers [see Fig. 2(a)]. As a result, only a small amount of matter needs to be removed to shape the fiber end into a microcone capable of generating Bessel-like beams [cf. Fig. 2(b)]. For a fiber tip already formed into a microball lens, the polishing phase to produce a FIMAX does not exceed 5 min and is reproducible. The scanning electron microscope (SEM) image of the FIMAX depicted in Fig. 2(c) shows that the proposed polishing technique allows the generation of well-defined conical interfaces over the fiber core area. Polished FIMAXs exhibit a sharp summit and a conical interface of high cosmetic quality. In this example, the cone apex is of subwavelength size with a radius of curvature of $\sim$175 nm. The effects of machining artifacts on the final shape of the microcone lens (rounded summit, scratches and digs on the conical surface) are sufficiently weak that they do not disturb the generation of the Bessel-like beams.

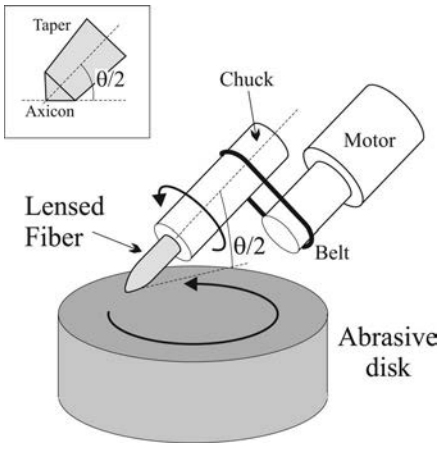

Fig. 1. Scheme of the polishing procedure. Inset, enlargement of the contact zone.

3. Bessel-like Beam 3D Imaging

The experimental setup developed for fully characterizing the 3D spatial behavior of the Bessel-like beams is depicted in Fig. 3. The imaging device consists of an inversed microscope, a piezoelectric 1D translation stage, and a CCD camera. The piezo system and the CCD camera are both driven by a computer for image acquisition. The optical fiber is attached parallel to the axis of the translation stage so that the FIMAX faces the objective and laser light (He–Ne laser, $\lambda = 632.8$ nm) is injected into the fiber from the free end.

The first step of the 3D image acquisition experiment consists of focusing the imaging system onto the apex of the FIMAX. For this task, the laser is switched off and the microcone is imaged in reflection mode while illuminated by the microscope halogen lamp. Although the cone summit is of subwavelength size, it can be located by detecting the corresponding diffraction spot in the CCD plane. This preliminary manipulation is essential to identify the location of the beginning of the Bessel-like beam in the measured 3D volume, just beyond the summit of the microcone. This focusing step is required because refraction of the fiber mode by the conical interface cannot be unambiguously detected by the imaging

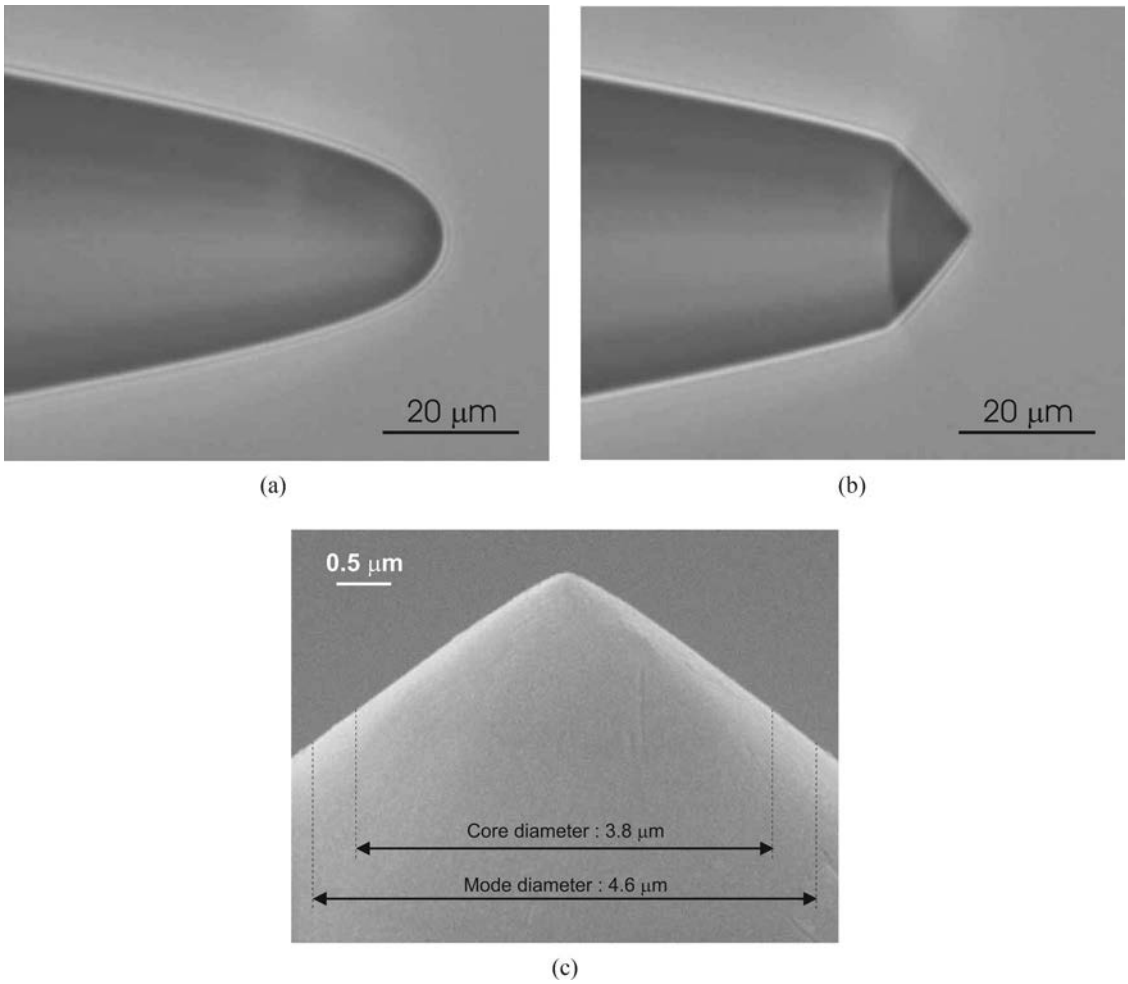

Fig. 2. Images of the fiber end after the two stages of the fabrication procedure developed in this study: (a) microball lens obtained by heating–pulling the fiber, (b) microaxicon obtained by polishing the microball lens, (c) SEM image of the polished FIMAX.

system. Therefore, if the objective were to be focused at a plane inside the fiber tip when the laser is switched on, the images would exhibit a light annulus larger than the fiber width. Although this annulus denotes the virtual extension along the fiber of the laminar conical beam inducing the Bessel-like beam, its appearance complicates the identification of the true beginning of the Bessel-like beam, just outside the conical tip.

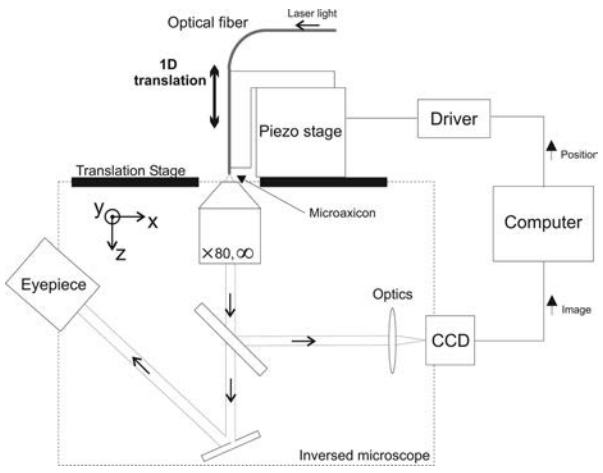

Fig. 3. Scheme of the acquisition setup.

For data acquisition, the microscope halogen lamp is switched off and the laser is switched on. The acquisition volume is obtained by moving the fiber step by step from the initial position previously defined. At each step, a 2D image is grabbed by a CCD camera and stored in the connected computer. The piezo stage ensures constant submicrometer displacements with a precision of the order of 1 nm. This slice-by-slice imaging process is stopped when the fiber end is sufficiently far from the objective that the Bessel beam vanishes. Finally, the set of images is combined to create a 3D acquisition volume.

To first approximation, Bessel-like beams transmitted through FIMAXs can be considered Bessel–Gauss beams. Such beams are accurately simulated by means of analytical methods [27]. However, these methods do not take into account the way the Bessel–Gauss beams are generated. In our case, such simulation methods cannot incorporate either the effects of refraction of the incident fiber mode

through the FIMAX or the effects of the longitudinal position of the FIMAX summit with respect to the beam on the spatial behavior of the resulting Bessel-like beam.

4. Results

Four polished FIMAXs of cone angles around 105°, 120°, 135°, and 150° (±2°) have been engineered at one of the two extremities of four pieces of the same type of optical fiber (one microcone lens per fiber piece). The chosen fiber (distributed by SEDI, Courcouronnes, France, model SMCA630B) is monomode for the He–Ne laser beam used in the experiments. The fundamental mode is here 4.6 μm wide (data provided by SEDI). Figure 4 displays both the longitudinal (*xz*) cross sections [Figs. 4(a), 4(c), 4(e), and 4(g)] and the transverse (*xy*) cross sections [Figs. 4(b), 4(d), 4(f), and 4(h)] of the Bessel-like beams generated by polished FIMAXs with cone angles of 150° [Figs. 4(a) and 4(b)], 135° [Figs. 4(c) and 4(d)], 120° [Figs. 4(e) and 4(f)], and 105° [Figs. 4(g) and 4(h)]. The transverse images are taken in the planes that contain the maximum intensity of the beams. In the following, those planes will be called (π) planes [locations marked with white arrows in Figs. 4(a), 4(c), 4(e), and 4(g)]. All images are displayed at the same scale for direct comparison of the 3D beam shapes, confinement abilities, and lengths for the different cone angles. The cone apex is located at $z = 0$ with a maximum uncertainty of ±2 μm when $\theta = 150°$.

First, we see that the Bessel-like beams obtained in all cases do not suffer from abberations and their confinement zones are well defined with good circular symmetry. This implies that the fabrication procedure described in this paper produces FIMAXs that are accurately centered with respect to the core axis, independent of the microcone angle. We estimate that the centration error does not exceed 1 μm. In

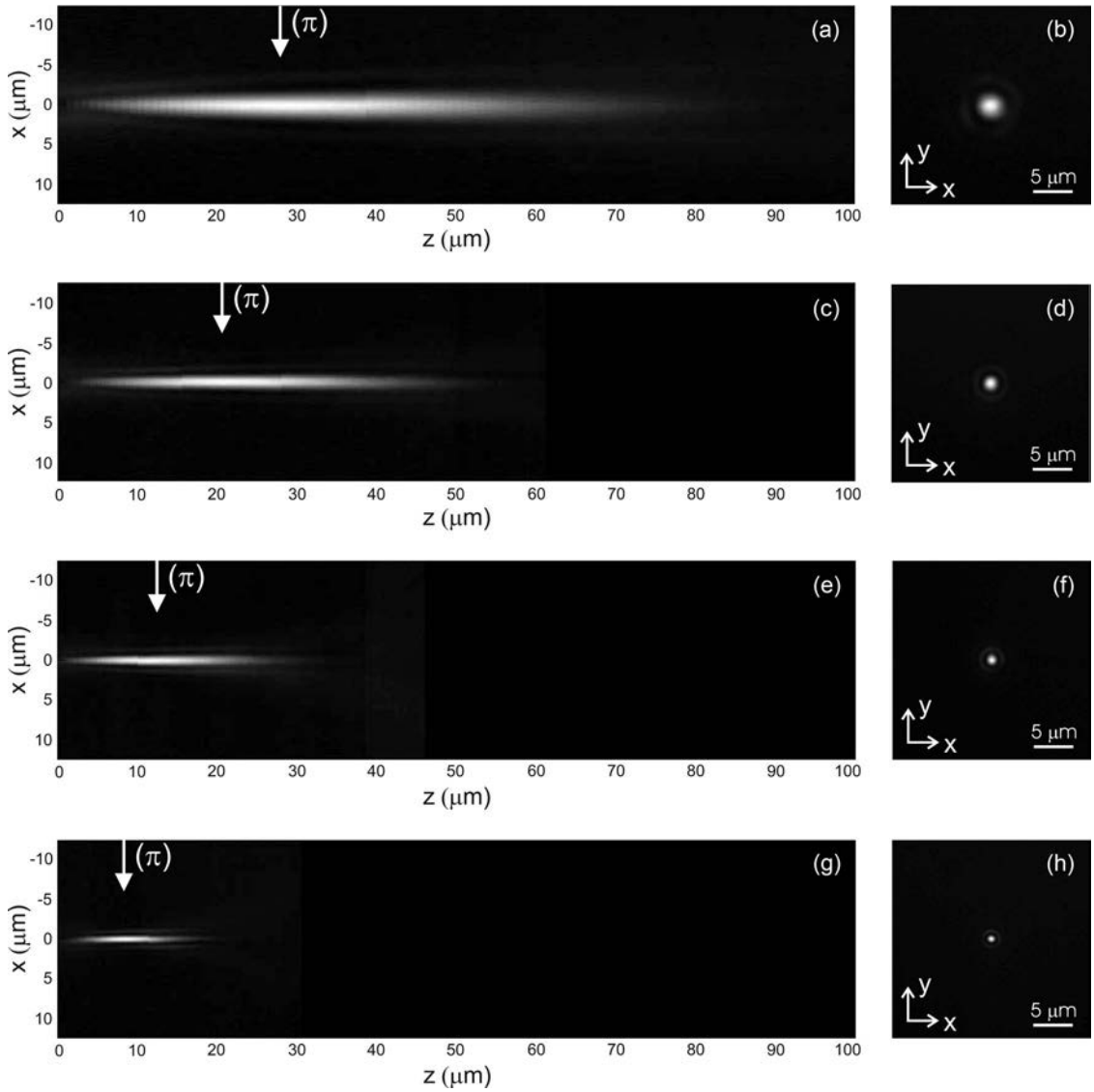

Fig. 4. (a), (c), (e), (g) Longitudinal (*xz*) and (b), (d), (f), (h) transverse (*xy*) cross sections of the Bessel-like beams generated for polished FIMAX angles of (a), (b) 150°, (c), (d) 135°, (e), (f) 120°, and (g), (h) 105°.

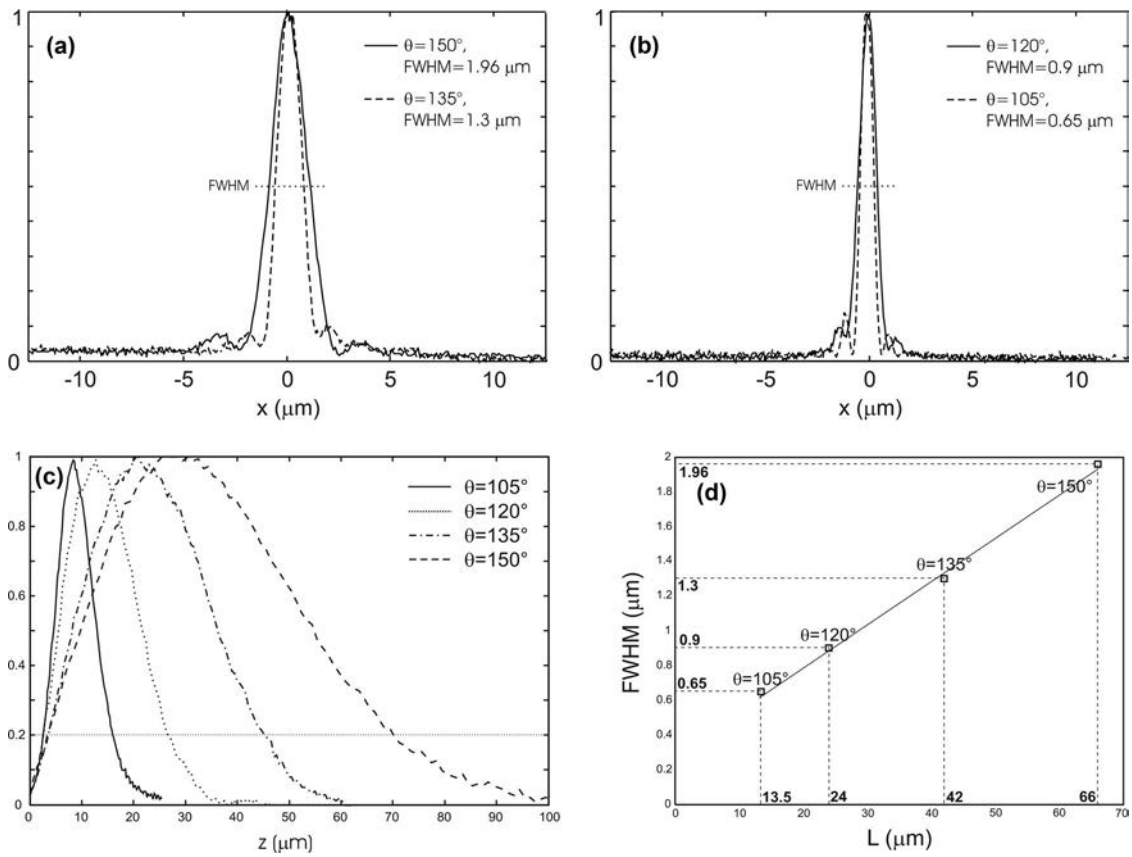

Fig. 5. (a), (b) Transverse intensity profiles and (c) longitudinal intensity profiles of the four Bessel-like beams generated by a polished FIMAX; (d) FWHM versus length.

addition, we see that the light distributions exhibit tubular spatial shapes, since the beam length is in all cases several times larger than the confinement zone. The low divergence of these light distributions confirms that these polished FIMAXs produce focused fields exhibiting spatial characteristics close to those of true Bessel beams, despite the diffraction phenomenon due to the limited size of the incident fiber mode. Finally, it appears that the reduction in spot size enabled by a larger FIMAX cone angle occurs at the expense of beam length.

The quantitative study of the beam dimensions is developed through Fig. 5. Figures 5(a) and 5(b) depict the Bessel-like beam profiles in the (π) plane, whereas Fig. 5(c) shows the longitudinal profiles along the beam axis of symmetry. The ability of the Bessel-like beams to confine light can be quantified by the FWHM of the intensity profiles depicted in Figs. 5(a) and 5(b). The length L of the Bessel-like beams is quantified from Fig. 5(c) as the distance over which the intensity along the beam axis is larger than 20% of the intensity maximum. The resulting dimensions of these Bessel-like beams are graphically reported in Fig. 5(d). When $\theta = 105°$, the confinement and the beam length are limited to 0.65 and 13.5 μm, respectively. These dimensions are increased to 0.9 and 24 μm when $\theta = 120°$, 1.3 and 42 μm when $\theta = 135°$, and, finally, 1.96 and 66 μm when $\theta = 150°$. The tubular shape of the beams is confirmed by the L-to-FWHM ratios, which range between 22.5 when $\theta = 105°$ and 33 when $\theta = 150°$. We note that the relationship between the confinement zone and the beam length can be regarded as being linear over the range of FIMAX angles considered here. Such a property allows the obvious estimation of the length of the Bessel-like beam for a given confinement zone, and conversely, the estimation of the confinement zone for a given beam length. For example, a confinement zone of 1 μm should lead to a beam length of 29 μm, whereas a beam length of 55 μm can be associated with a confinement zone of 1.63 μm. Therefore, Fig. 5(d) can be used as a simple means to calibrate the confinement zone versus the beam length. Note that the linear relationship between L and the size of the confinement zone can be explained by our definition of these parameters.

The differences between the spatial behaviors of an ideal Bessel beam and those generated at the extremity of an optical fiber can be explained qualitatively through the study of their angular spectra. In the ideal case, the angular spectrum of a Bessel beam is defined by a circle that leads to the nondiffracting properties of the beam. In our case, the angular spectrum resembles an annulus whose width is set by the lateral extension of the incident fiber mode. The broader the fiber mode, the narrower the annulus, and thus, the closer the output beam approaches the ideal Bessel beam. The ring-shaped angular spec-

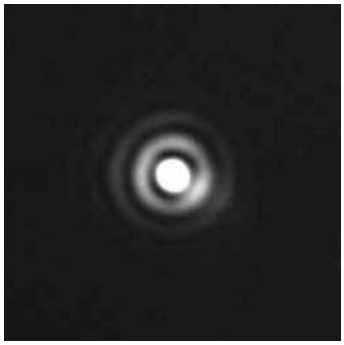

Fig. 6. Saturated transverse cross section of a Bessel-like beam generated with a microaxicon of 120° cone angle.

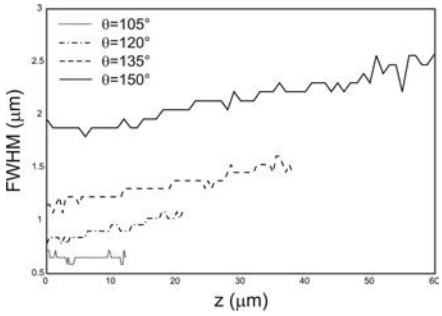

Fig. 8. FWHM of the transverse light distribution as a function of the longitudinal distance from the FIMAX summit.

trum can be seen in the direct space as the coherent combination of ideal Bessel beams of various wave vectors. This interference phenomenon is constructive at the center of the resulting Bessel-like beam since all the positive maxima of the various Bessel beam central lobes are constructively added. The combination of the Bessel beam lateral lobes of different periodicities leads to a destructive interference phenomenon in the region surrounding the central light confinement. Such properties have several effects on the spatial behavior of the global Bessel-like beam. First, the lateral lobes are strongly attenuated compared with those of the ideal Bessel beams. We see for instance in Fig. (6) that only three lateral fringes are clearly visible around the central spot in the saturated image of the Bessel-like beam generated with a fiber axicon of 120° cone angle.

Second, the confinement ability of the Bessel-like beam is a little lower than that of the ideal Bessel beams, which can be described in first approximation by the Bessel function J_0 [2]. Figure (7) displays the Bessel-like beam spatial characteristics (FWHM and length L) as functions of the FIMAX numerical aperture (NA).

Figure 7(a) shows that the spot size of the Bessel-like beam is systematically larger than that of the ideal Bessel beam, whatever the NA. Such a discrepancy is due to the constructive combination of the central lobes (of different sizes) of the ideal Bessel beams that constitute the Bessel-like beam. Finally, the confinement zone widens slightly as the longitudinal distance (z) from the FIMAX summit increases. Figure (8) shows that the measured confinement zone is broadened over the propagation distance of the Bessel-like beam by 0.7 μm when θ = 150°, 0.37 μm when θ = 135°, and 0.25 μm when θ = 120° but remains roughly constant for θ = 105°. Such low divergence properties prove that the polished FIMAX is a promising solution for generating a tiny stylus of light for many applications.

5. Conclusion

This paper has been devoted to the presentation of an alternative method, based on a polishing technique, for generating fiber-integrated microaxicons. This solution has the advantage of being simple, low cost, and rapid (fabrication durations of a few minutes). As a result, the FIMAX angle can be chosen in a straightforward and versatile way simply by choosing

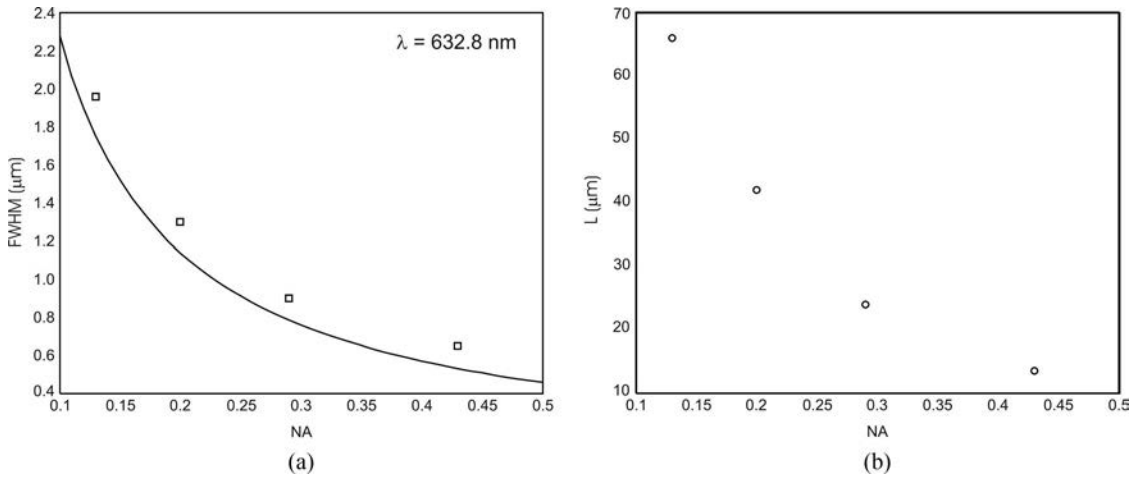

Fig. 7. (a) Comparison between the confinement zones of the experimental Bessel-like beams [FWHM of the intensity distribution in (π) plane, squares] and those created by an ideal Bessel beam (FWHM of function J_0^2, solid curve). (b) Length L of the Bessel-like beam (depth of field) as a function of the FIMAX NA.

the right tilt angle of the optical fiber with respect to the abrasive disk during polishing. We have studied the spatial behavior of the Bessel-like beams for four different polished FIMAX cone angles using measured 3D light distributions. This quantitative study of the beam dimensions reveals a linear relationship between the length and transverse width of the Bessel-like beam confinement zone. This result allows one to directly define *a priori* the spatial dimensions of the field distributions to be produced by a FIMAX, according to the particular application requirements. Finally, we have shown experimentally that the effects of diffraction on the studied Bessel-like beams are mainly the attenuation of the lateral fringes, a small loss of confinement ability (with respect to the ideal Bessel beam), and finally a slight broadening of the confinement zone with propagation distance. Given their ease of fabrication and near-Bessel-beam optical performance, FIMAXs fabricated by polishing techniques are promising compact systems for creating a tiny stylus of light usable in various domains of growing interest such as micro- and nano-optics, laser surgery, endoscopy, data storage, scanning microscopy, optical tweezers, and beyond.

The authors are indebted to R. Giust for his help and support in the use of the detection setup for the Bessel beam 3D imaging. They also thank Geoffrey Burr for his helpful advice in the writing of the manuscript.

References

1. J. Durnin, "Exact solutions for nondiffracting beams. I. The scalar theory," J. Opt. Soc. Am. A **4,** 651–654 (1987).
2. J. Durnin, J. J. Miceli, and J. H. Eberly, "Diffraction-free beams," Phys. Rev. Lett. **58,** 1499–1501 (1987).
3. B. Hafizi, E. Esarey, and P. Sprangle, "Laser-driven acceleration with Bessel beams," Phys. Rev. E. **55,** 3539–3545 (1997).
4. S. C. Tidwell, D. H. Ford, and W. D. Kimura, "Transporting and focusing radially polarized laser beams," Opt. Eng. **31,** 1527–1531 (1992).
5. J. Arlt, K. Dholakia, J. Soneson, and E. M. Wright, "Optical dipole traps and atomic waveguides based on Bessel light beams," Phys. Rev. A **63,** 1–8 (2001).
6. V. Garces-Chavez, D. McGloin, H. Melville, W Sibbett, and K. Dholakia, "Simultaneous micromanipulation in multiple planes using self-reconstructing light beam," Nature (London) **419,** 145 (2002).
7. J. Arlt, V. Garces-Chavez, W. Sibbett, and K. Dholakia, "Optical micromanipulation using a Bessel light beam," Opt. Commun. **197,** 239–245 (2001).
8. T. Wulle and S. Herminghaus, "Nonlinear optics of Bessel beams," Phys. Rev. Lett. **70,** 1401–1405 (1993).
9. K. Shinozaki, C. Xu, H. Sasaki, and T. Kamijoh, "A comparison of optical second-harmonic generation efficiency using Bessel and Gaussian beams in bulk crystals," Opt. Commun. **133,** 300–304 (1997).
10. A. Piskarskas, V. Smilgevicius, V. Jarutis, V. Pasiskevicius, S. Wang, J. Tellefsen, and F. Laurell, "Noncollinear second-harmonic generation in periodically poled $KtiOPO_4$ excited by the Bessel beam," Opt. Lett. **24,** 1053–1055 (1999).
11. V. Jarutis, A. Matijosius, V. Smilgevicius, and A. Stabinis, "Second harmonic generation of higher-order Bessel beams," Opt. Commun. **185,** 159–169 (2000).
12. V. E. Peet and R. V. Tsubin, "Third-harmonic generation and multiphoton ionization in Bessel beams," Phys. Rev. A **56,** 1613–1620 (1997).
13. V. N. Belyi, N. S. Kazak, and N. A. Khilo, "Properties of parametric frequency conversion with Bessel light beams," Opt. Commun. **162,** 169–176 (1999).
14. S. Klewitz, S. Sogomonian, M. Woerner, and S. Herminghaus, "Stimulated Raman scattering of femtosecond Bessel pulses," Opt. Commun. **154,** 186–190 (1998).
15. R. P. MacDonald, S. A. Boothroyd, T. Okamoto, J. Chrostowski, and B. A. Syrett, "Interboard optical data distribution by Bessel beam shadowing," Opt. Commun. **122,** 169–177 (1996).
16. C. Yu, M. R. Wang, A. J. Varela, and B. Chen, "High-density non-diffracting beam array for optical interconnection," Opt. Commun. **177,** 369–376 (2000).
17. R. Arimoto, C. Saloma, T. Tanaka, and S. Kawata, "Imaging properties of axicon in a scanning optical system," Appl. Opt. **31,** 6653–6657 (1992).
18. A. Marcinkevicius, S. Juodkazis, S. Matsuo, V. Mizeikis, and H. Misawa, "Application of Bessel beams for microfabrication of dielectrics by femtosecond laser," Jpn. J. Appl. Phys. **40,** 1197–1199 (2001).
19. M. Erdelyi, Z. L. Horvath, G. Szabo, Zs. Bor, F. K. Tittel, J. R. Cavallaro, and M. C. Smayling, "Generation of diffraction-free beams for application in optical microlithography," J. Vac. Sci. Technol. B **15,** 287–292 (1997).
20. J. H. McLeod, "Axicons and their uses," J. Opt. Soc. Am. **50,** 166–169 (1960).
21. R. M. Herman and T. A. Wiggins, "Production and uses of diffractionless beams," J. Opt. Soc. Am. A **8,** 932–942 (1991).
22. G. Scott and N. McArdle, "Efficient generation of nearly diffraction-free beams using an axicon," Opt. Eng. **31,** 2640–2643 (1992).
23. G. Eisenstein and D. Vitello, "Chemically etched conical microlenses for coupling single-mode lasers into single-mode fibers," Appl. Opt. **21,** 3470–3474 (1982).
24. S.-K. Eah and W. Jhe, "Nearly diffraction-limited focusing of a fiber axicon microlens," Rev. Sci. Instrum. **74,** 4969–4971 (2003).
25. S. Cabrini, C. Liberale, D. Cojoc, A. Carpentiero, M. Prasciolu, S. Mora, V. Degiorgio, F. De Angelis, and E. Di Fabrizio, "Axicon lens on optical fiber forming optical tweezers, made by focused ion beam milling," Microelectron. Eng. **83,** 804–807 (2006).
26. T. Held, S. Emonin, O. Marti, and O. Hollricher, "Method to produce high-resolution scanning near-field optical microscope probes by beveling optical fibers," Rev. Sci. Instrum. **71,** 3118–3122 (2000).
27. F. Gori, G. Guattari, and C. Padovani, "Bessel–Gauss beams," Opt. Commun. **64,** 491–495 (1987).